Quantum reading of quantum information

OPEN ACCESS
IOP Publishing
Journal of Physics A: Mathematical and Theoretical
J. Phys. A: Math. Theor. **56** (2023) 485302 (16pp)
https://doi.org/10.1088/1751-8121/ad075f

Quantum reading of quantum information

Samad Khabbazi Oskouei[1], **Stefano Mancini**[2,3] and **Milajiguli Rexiti**[2,3,*]

[1] Department of Mathematics, Varamin-Pishva Branch, Islamic Azad University, Varamin 33817-7489, Iran
[2] School of Science and Technology, University of Camerino, Via Madonna delle Carceri 9, I-62032 Camerino, Italy
[3] INFN-Sezione di Perugia, Via A. Pascoli, I-06123 Perugia, Italy

E-mail: milajiguli.milajiguli@unicam.it

Received 24 July 2023; revised 18 October 2023
Accepted for publication 26 October 2023
Published 8 November 2023

Abstract

We extend the notion of quantum reading to the case where the information to be retrieved, which is encoded into a set of quantum channels, is of quantum nature. We use two-qubit unitaries describing the system-environment interaction, with the initial environment state determining the system's input-output channel and hence the encoded information. The performance of the most relevant two-qubit unitaries is determined with two different approaches: (i) one-shot quantum capacity of the channel arising between environment and system's output; (ii) estimation of parameters characterizing the initial quantum state of the environment. The obtained results are mostly in (qualitative) agreement, with some distinguishing features that include the CNOT unitary.

Keywords: quantum reading, quantum fisher information, one-shot quantum channel capacity

1. Introduction

Quantum reading is the process of retrieving classical information from a memory by using a quantum probe [1] (for a survey on the subject see [2]). It is customary to see such information encoded into a finite set of quantum channels, each one labeled by the value that a random discrete variable can take. As a such, the process involves quantum channel discrimination [3–6]. Quantum reading has been applied in various contexts, ranging from physical imaging

* Author to whom any correspondence should be addressed.

[7], to radar [8], to biology [9], to cryptography [10], and showed advantages over classical reading.

A prototypical model for a memory cell in quantum reading is the environment parametrized quantum channel [11–15]. This is a unitary acting on two systems: the main system and the environment. Depending on the state of the latter, a channel can be realized on the former by tracing out the environment at the end. Thus, the initial state of the environment can be considered as the encoded information that has to be retrieved, while the main system plays the role of the probe. This model was custumarily employed with environment input states forming an orthonormal basis for the associated Hilbert space. In such a way it realized an incoherent model of memory cell (investigated also for private reading [16]).

Here, we do not restrict the input quantum states of the environment to be discrete or even orthogonal. Instead, we consider any possible state on the associated Hilbert space with the goal of determining it. This seems to us the most natural way to look at quantum reading of quantum information, or in other words at the quantum communication between encoder and reader. That is inline with the coherent model of memory cell (allowing for entanglement generation between encoder and reader) put forward in [17] by resorting to conditional operations. However, we shall consider generic unitaries together with generic environment states, rather than conditional unitaries together with specific environment states. Furthermore, we shall focus on finite (or even single) use of the channel connecting the environment with the output of the main system (probe), rather than on its asymptotic behavior. In fact quantum information has to be extracted with a finite number of usage of the channel realized on the main system (probe) and a nonzero probability of error. Then, as a figure of merit we resort to the one-shot quantum capacity [18]. Since explicit computation of one-shot capacity is challenging, we shall compute a lower bound on it following [19]. Additionally, we shall consider the information to be retrieved as residing on the parameters characterizing the encoded quantum state, thus tracing back the problem to continuous multi-parameter estimation. In this case as figure of merit we shall consider a Bayesian version of the quantum Cramer–Rao bound derived from the classical bound [20]. We shall confine our attention to two-qubit unitaries. In particular those that are entangling. These can be represented by points lying in a tetrahedron in $\mathbb{R}^3$ (see e.g. [21]). Specifically, we characterize the quantum reading of quantum information on the edges of this tetrahedron starting from its vertices. The found results show a large qualitative agreement between the approach based on the one-shot quantum capacity bound and the approach based on Bayesian quantum Cramer–Rao bound, with some distinguishing features that include the CNOT unitary.

The paper is organized as follows. In section 2 we introduce the model and state the problem to deal with. In section 3 we study the one-shot quantum capacity by evaluating a lower bound for relevant two-qubit unitaries. Then, in section 4 we study the quantum state estimation by evaluating on the same unitaries a Bayesian version of the Cramer–Rao bound. Finally in section 5 we draw our conclusions.

2. The model

Consider a unitary $U^{AE\to BF}$ with systems $A \simeq B$ and $E \simeq F$ (here, with little abuse of notation, the system's label also denotes the associated Hilbert space). By referring to figure 1, the environment parametrization of quantum channel [11–15] consists in characterizing a channel $\mathcal{N}_\theta^{A\to B}$ between A and B in terms of the E state $\boldsymbol{\theta}$.

For the purpose of quantum reading systems A and B, i.e. input and output of $\mathcal{N}_\theta^{A\to B}$, are both held by the reader, which wants to retrieve the state $\boldsymbol{\theta}$ of the system E. It is customary

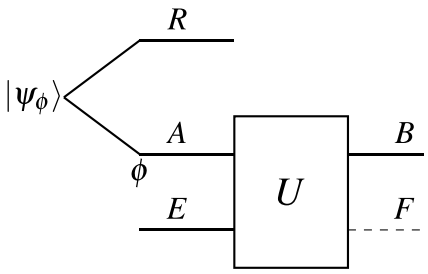

Figure 1. General model for quantum reading based on environment parametrization of quantum channels. $|\psi_\phi\rangle$ is the purification of the input ϕ to the A system.

to consider $x \in \mathscr{X}$ (discrete and finite alphabet) encoded by E as orthogonal states $|x\rangle$ with probability p_x. Then, the objective for the reader, given $\mathscr{N}_x^{A\to B}$, is to find x among all possible values in $\mathscr{X}$. This task can give rise to classical communication [22] as well as to quantum communication [17] between E and B.

In fact, for classical information transmission, an incoherent picture is used leading to the final state of the whole system as

$$U\left(|\psi_\phi\rangle\langle\psi_\phi| \otimes \sum_x p_x|x\rangle\langle x|\right)U^\dagger. \tag{1}$$

Instead, for quantum information transmission, a coherent picture is used leading to the final state of the whole system as

$$\sum_x \sqrt{p_x}\,(V^x|\psi_\phi\rangle)\,|x\rangle, \tag{2}$$

where it is assumed $U = \sum_x V^x \otimes |x\rangle\langle x|$ applied to an environment state $\sum_x \sqrt{p_x}|x\rangle$.[4]

Here we change the paradigm and according to figure 1 we consider a generic unitary U together with a generic state $\boldsymbol{\theta}$ encoded into E. Then the objective is to recover such a state. This of course implies the necessity of transmitting quantum information from E to B or alternatively the necessity of estimating the environment state.

We will focus on two-qubit unitaries $U^{AE\to BF}$, with states $\boldsymbol{\phi}, \boldsymbol{\theta}$ on A and E systems respectively. The former is the input of the probe system and the latter the encoded state in the memory. The bold symbols emphasize that the qubit states are characterized by vectors of $\mathbb{R}^3$.

Two-qubit entangling unitaries that can be written as [24]

$$U^{AE\to BF} = \sum_{k=1}^{4} e^{-i\lambda_k}|\Lambda_k\rangle\langle\Lambda_k|, \tag{3}$$

where $|\Lambda_k\rangle$ are the so called magic basis states:

[4] This picture was then extended to coherent quantum channel discrimination [23].

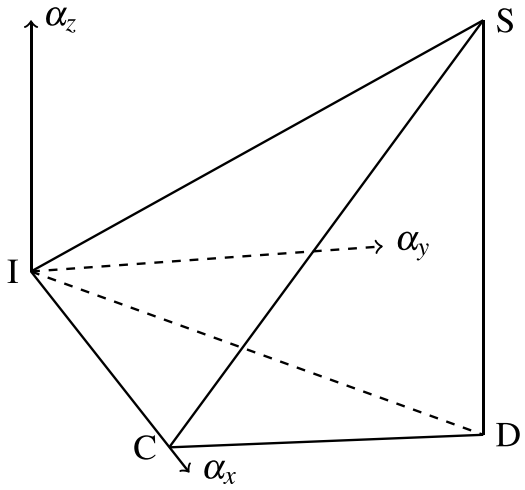

Figure 2. Tetrahedron representing the parameters space of two-qubit unitaries, where I, C, S, D stand for Identity, CNOT, SWAP and DCNOT unitaries respectively.

$$|\Lambda_1\rangle = \frac{1}{\sqrt{2}}\left(|0\rangle_A|0\rangle_E + |1\rangle_A|1\rangle_E\right), \qquad |\Lambda_2\rangle = \frac{-i}{\sqrt{2}}\left(|0\rangle_A|0\rangle_E - |1\rangle_A|1\rangle_E\right),$$
$$|\Lambda_3\rangle = \frac{1}{\sqrt{2}}\left(|0\rangle_A|1\rangle_E - |1\rangle_A|0\rangle_E\right), \qquad |\Lambda_4\rangle = \frac{-i}{\sqrt{2}}\left(|0\rangle_A|1\rangle_E + |1\rangle_A|0\rangle_E\right), \tag{4}$$

and the eigenvalues λ_k are

$$\lambda_1 = \frac{\alpha_x - \alpha_y + \alpha_z}{2}, \qquad \lambda_2 = \frac{-\alpha_x + \alpha_y + \alpha_z}{2},$$
$$\lambda_3 = \frac{-\alpha_x - \alpha_y - \alpha_z}{2}, \qquad \lambda_4 = \frac{\alpha_x + \alpha_y - \alpha_z}{2}, \tag{5}$$

with

$$\frac{\pi}{2} \geqslant \alpha_x \geqslant \alpha_y \geqslant \alpha_z \geqslant 0. \tag{6}$$

In the canonical basis $\{|0\rangle_A|0\rangle_E, |0\rangle_A|1\rangle_E, |1\rangle_A|0\rangle_E, |1\rangle_A|1\rangle_E\}$ we have

$$U = \begin{pmatrix} \cos\left(\frac{\alpha_x-\alpha_y}{2}\right) & 0 & 0 & -i\sin\left(\frac{\alpha_x-\alpha_y}{2}\right) \\ 0 & e^{i\alpha_z}\cos\left(\frac{\alpha_x+\alpha_y}{2}\right) & -ie^{i\alpha_z}\sin\left(\frac{\alpha_x+\alpha_y}{2}\right) & 0 \\ 0 & -ie^{i\alpha_z}\sin\left(\frac{\alpha_x+\alpha_y}{2}\right) & e^{i\alpha_z}\cos\left(\frac{\alpha_x+\alpha_y}{2}\right) & 0 \\ -i\sin\left(\frac{\alpha_x-\alpha_y}{2}\right) & 0 & 0 & \cos\left(\frac{\alpha_x-\alpha_y}{2}\right) \end{pmatrix}. \tag{7}$$

All unitaries of this kind form, according to equation (6), a tetrahedron in the parameter space $\alpha_x, \alpha_y, \alpha_z$ (see figure 2). The vertices of such a tetrahedron represent Identity, SWAP, CNOT and DCNOT unitaries.

3. One-shot quantum capacity

By referring to figure 1, for a fixed probe state ϕ, we can consider the channel

$$\mathcal{N}_{\phi}^{E\to B}(\boldsymbol{\theta}) = \mathrm{Tr}_F\left(U^{AE\to BF}\left(\phi\otimes\boldsymbol{\theta}\right)\left(U^{AE\to BF}\right)^{\dagger}\right), \tag{8}$$

and evaluate its capability in transmitting quantum information. In particular, we are interested to the one-shot quantum capacity for the channel $\left(\mathcal{N}_{\phi}^{E\to B}(\boldsymbol{\theta})\right)^{\otimes n}$. This will tell us how much quantum information we can extract from system E^n by accessing system B^n in one shot and with a finite probability of error.

3.1. Lower bound

Notice preliminarily that the complementary channel of $\mathcal{N}_{\phi}^{E\to B}(\boldsymbol{\theta})$ reads

$$\left(\mathcal{N}_{\phi}^{E\to B}\right)^{c}(\boldsymbol{\theta}) = \mathrm{Tr}_B\left(U^{AE\to BF}\left(\phi\otimes\boldsymbol{\theta}\right)\left(U^{AE\to BF}\right)^{\dagger}\right). \tag{9}$$

Let us also set

$$\rho_{BF} := \left(\mathrm{id}^{A\to B}\otimes\left(\mathcal{N}_{\phi}^{E\to B}\right)^{c}\right)(\Phi_{AE}), \tag{10}$$

where Φ_{AE} is maximally entangled state across the systems A and E. In this way we will deal with the Choi matrix of the channel $(\mathcal{N}_{\phi}^{E\to B})^{c}$. Analogously, it will be

$$\rho_{B^nF^n} := \left(\mathrm{id}^{A^n\to B^n}\otimes\left(\left(\mathcal{N}_{\phi}^{E\to B}\right)^{c}\right)^{\otimes n}\right)(\Phi_{A^nE^n}), \tag{11}$$

with $\Phi_{A^nE^n}$ a maximally entangled state across the systems A^n and E^n.

For a given $\varepsilon>0$, the one-shot quantum capacity of $\left(\mathcal{N}_{\phi}^{E\to B}\right)^{\otimes n}$ results as [18]

$$Q^{\varepsilon}\left(\left(\mathcal{N}_{\phi}^{E\to B}\right)^{\otimes n}\right) = \max\left\{\log_2 m \,|\, F_{\min}\left(\left(\mathcal{N}_{\phi}^{E\to B}\right)^{\otimes n}, m\right)\geqslant 1-\varepsilon\right\}, \tag{12}$$

where

$$F_{\min}\left(\left(\mathcal{N}_{\phi}^{E\to B}\right)^{\otimes n}, m\right) := \max_{\substack{\mathscr{H}_E'\subset\mathscr{H}_E^n,\\ \dim\left(\mathcal{H}_E'\right)=m}}\ \max_{\mathcal{D}}\ \min_{|\omega\rangle\in\mathscr{H}_E'}\langle\omega|\left(\mathscr{D}\circ\left(\mathcal{N}_{\phi}^{E\to B}\right)^{\otimes n}\right)(\omega)\,|\omega\rangle. \tag{13}$$

Here $\mathscr{D}$ is a decoding map from $\mathscr{H}_B^n\simeq\mathscr{H}_E^n$ to $\mathscr{H}_B'\simeq\mathscr{H}_E'$.

A lower bound to (12) is given as follows [19]

$$Q^{\varepsilon}\left(\left(\mathcal{N}_{\phi}^{E\to B}\right)^{\otimes n}\right)\geqslant \sup_{\delta\in\left(0,\sqrt{\varepsilon/2}\right)}\left(H_{\min}^{\sqrt{\varepsilon/2}-\delta}\left(B^n|F^n\right)_{\rho^n} - 4\log_2\frac{1}{\delta} - 2\right). \tag{14}$$

It is

$$H_{\min}^{\varepsilon}\left(B^n|F^n\right)_{\rho^n} := \max_{\rho'_{B^nF^n}\in\mathscr{B}^{\varepsilon}\left(\rho_{B^nF^n}\right)} H_{\min}\left(B^n|F^n\right)_{\rho'_{B^nF^n}}, \tag{15}$$

where

$$\mathscr{B}^{\varepsilon}\left(\rho_{B^nF^n}\right) = \left\{\rho'_{B^nF^n}\,|\,\mathrm{tr}\left(\rho'_{B^nF^n}\right)\leqslant 1, \sqrt{1-F\left(\rho_{B^nF^n},\rho'_{B^nF^n}\right)}\leqslant\varepsilon\right\}, \tag{16}$$

with

$$F\left(\rho_{B^nF^n},\rho'_{B^nF^n}\right) := \left\|\sqrt{\rho_{B^nF^n}}\sqrt{\rho'_{B^nF^n}}\right\|_1^2. \tag{17}$$

Furthermore

$$H_{\min}\left(B^n|F^n\right)_{\rho^n} = \max_{\sigma_{F^n}} \sup\left\{\lambda \in \mathbb{R} | \, \rho_{B^nF^n} \leqslant 2^{-\lambda} I_{B^n} \otimes \sigma_{F^n}\right\}, \tag{18}$$

with $\rho_{B^nF^n}$ given by (11).

We also have the following inequality for $\alpha \in (1,\infty)$ [25]

$$H^{\varepsilon}_{\min}\left(B^n|F^n\right)_{\rho^n} \geqslant \mathbb{H}_q\left(B^n|F^n\right)_{\rho^n} - \frac{g\left(\varepsilon\right)}{q-1}, \tag{19}$$

being

$$g\left(\varepsilon\right) := -\log_2\left(1-\sqrt{1-\varepsilon^2}\right). \tag{20}$$

Here $\mathbb{H}_q$ is the conditional Renyi entropy, which is defined as

$$\mathbb{H}_q\left(B^n|F^n\right)_{\rho^n} := \max_{\sigma_{F^n}} -D_q\left(\rho_{B^nF^n}\|I_{B^n}\otimes\sigma_{F^n}\right), \tag{21}$$

with

$$D_q\left(\rho_{B^nF^n}\|I_{B^n}\otimes\sigma_{F^n}\right) := \frac{1}{q-1}\log_2 \mathrm{Tr}\left\{\left[\left(I_{B^n}\otimes\sigma_{F^n}\right)^{\frac{1-q}{2q}}\rho_{B^nF^n}\left(I_{B^n}\otimes\sigma_{F^n}\right)^{\frac{1-q}{2q}}\right]^q\right\}. \tag{22}$$

Considering $q=2$, by combining relations (14) and (19), we have

$$Q^{\varepsilon}\left(\left(\mathscr{N}_{\phi}^{E\to B}\right)^{\otimes n}\right) \geqslant \sup_{\delta\in\left(0,\sqrt{\varepsilon/2}\right)}\left[\mathbb{H}_2\left(B^n|F^n\right)_{\rho^n} - g\left(\sqrt{\frac{\varepsilon}{2}}-\delta\right) - 4\log_2\frac{1}{\delta} - 2\right]. \tag{23}$$

By restricting the attention to product states $\sigma_{F^n} = \sigma_F^{\otimes n}$ and $\rho_{B^nF^n} = \rho_{BF}^{\otimes n}$ in $\mathbb{H}_2(B^n|F^n)_{\rho^n}$ and using $\mathbb{H}_2(B^n|F^n)_{\rho^{\otimes n}} \geqslant n\mathbb{H}_2(B|F)_{\rho}$, we finally arrive to

$$\begin{aligned} Q^{\varepsilon,n}\left(\mathscr{N}_{\phi}^{E\to B}\right) &:= \frac{1}{n}Q^{\varepsilon}\left(\left(\mathscr{N}_{\phi}^{E\to B}\right)^{\otimes n}\right) \\ &\geqslant \sup_{\delta\in\left(0,\sqrt{\varepsilon/2}\right)}\left[\mathbb{H}_2\left(B|F\right)_{\rho} - \frac{1}{n}\left(g\left(\sqrt{\frac{\varepsilon}{2}}-\delta\right) + 4\log_2\frac{1}{\delta} + 2\right)\right] \\ &= \mathbb{H}_2\left(B|F\right)_{\rho} - \frac{1}{n}\left(g\left(\sqrt{\frac{\varepsilon}{2}}-\delta_{\star}\right) + 4\log_2\frac{1}{\delta_{\star}} + 2\right), \end{aligned} \tag{24}$$

where $\delta_{\star}$ is the value of δ minimizing the expression $g\left(\sqrt{\varepsilon/2}-\delta\right) - 4\log_2\delta$ within the interval $(0,\sqrt{\varepsilon/2})$ (see appendix A).

3.2. Evaluation on the vertices

We now work out the calculation of the r.h.s. of (24) for the four cases of unitaries in the vertices of tetrahedron (see figure 2).

(i) $\alpha_x = \alpha_y = \alpha_z = 0$ $(U = I)$. In this case $\rho_{BF} = \Phi_{AE}$. Then, we have

$$\mathbb{H}_2\left(B|F\right)_{\rho} = -\min_{\sigma_F}\log_2\mathrm{Tr}\left\{\left(\left(I_B\otimes\sigma_F\right)^{-\frac{1}{2}}\Phi_{AE}\right)^2\right\} \tag{25}$$

$$\leqslant -\log_2\mathrm{Tr}\left\{\left(\Phi_{AE}\right)^2\right\} \leqslant 0. \tag{26}$$

Therefore the lower bound (24) trivially becomes zero.

(ii) $\alpha_x = \frac{\pi}{2}$, $\alpha_y = \alpha_z = 0$ ($U = CNOT$). In this case

$$\rho_{BF} = \frac{1}{4}\begin{pmatrix} 1 & i\sin(2\phi_1)\cos\phi_2 & \sin(2\phi_1)\sin\phi_2 & 1 \\ -i\sin(2\phi_1)\cos\phi_2 & 1 & 1 & -\sin(2\phi_1)\sin\phi_2 \\ -\sin(2\phi_1)\sin\phi_2 & 1 & 1 & -\sin(2\phi_1)\cos\phi_2 \\ 1 & i\sin(2\phi_1)\sin\phi_2 & i\sin(2\phi_1)\cos\phi_2 & 1 \end{pmatrix}. \tag{27}$$

Let us set $\eta_F := \sqrt{\sigma_F}/\mathrm{Tr}\sqrt{\sigma_F}$ and assume that λ_1 and λ_2 are eigenvalues of σ_F with

$$\eta_F = \frac{1}{2}\begin{pmatrix} 1+r_3 & r_1 - ir_2 \\ r_1 + ir_2 & 1-r_3 \end{pmatrix}, \quad \sigma_F = \frac{1}{2}\begin{pmatrix} 1+p_3 & p_1 - ip_2 \\ p_1 + ip_2 & 1-p_3 \end{pmatrix}. \tag{28}$$

We have

$$\mathbb{H}_2(B|F)_\rho = \max_{\sigma_F}\left(-\log_2 \mathrm{Tr}\left\{\left((I_B\otimes\sigma_F)^{-\frac{1}{2}}\rho_{BF}\right)^2\right\}\right) \tag{29}$$

$$= -\min_{\sigma_F}\log_2 \frac{\mathrm{Tr}\left\{\left((I_B\otimes\eta_F)^{-1}\rho_{BF}\right)^2\right\}}{\left(\mathrm{Tr}\sqrt{\sigma_F}\right)^2} \tag{30}$$

$$= -\min_{\sigma_F}\log_2 \frac{2\left(1+r_1^2+\left(1-r_1^2\right)\cos^2\phi_1\cos^2\phi_2\sin^2(2\phi_1)\right)}{\left(\mathrm{Tr}\sqrt{\sigma_F}\right)^2\left(1-r_1^2-r_2^2-r_3^2\right)^2} \tag{31}$$

$$\leqslant -\min_{\sigma_F}\log_2 \frac{1+r_1^2}{8\left(\left(\mathrm{Tr}\sqrt{\sigma_F}\right)^2\det(\eta_F)\right)^2} \tag{32}$$

$$= -\min_{\sigma_F}\log_2 \frac{\left(\mathrm{Tr}\sqrt{\sigma_F}\right)^2\left(1+r_1^2\right)}{8\det(\sigma_F)} \tag{33}$$

$$= \max_{\sigma_F} -\log_2 \frac{\left(\sqrt{\lambda_1}+\sqrt{\lambda_2}\right)^2\left(1+r_1^2\right)}{8\lambda_1\lambda_2} \tag{34}$$

$$\leqslant -\min_{\sigma_F}\log_2 \frac{\left(1+2\sqrt{\lambda_1\lambda_2}\right)\left(1+r_1^2\right)}{8\lambda_1\lambda_2} \leqslant 0. \tag{35}$$

For the last inequality we used the fact that $1+2\sqrt{x(1-x)} \geqslant 8x(1-x)$ for $0 \leqslant x \leqslant 1$. Again the lower bound (24) trivially becomes zero.

(iii) $\alpha_x = \alpha_y = \alpha_z = \frac{\pi}{2}$ ($U = SWAP$). In this case

$$\rho_{BF} = \begin{pmatrix} \frac{1}{2}\cos^2(\phi_1) & \frac{1}{4}e^{i\phi_2}\sin(2\phi_1) & 0 & 0 \\ \frac{1}{4}e^{-i\phi_2}\sin(2\phi_1) & \frac{1}{2}\sin^2(\phi_1) & 0 & 0 \\ 0 & 0 & \frac{1}{2}\cos^2(\phi_1) & -\frac{1}{4}e^{i\phi_2}\sin(2\phi_1) \\ 0 & 0 & \frac{1}{4}e^{-i\phi_2}\sin(2\phi_1) & \frac{1}{2}\sin^2(\phi_1) \end{pmatrix}. \tag{36}$$

This can also be written as $\rho_{BF} = \frac{I}{2}\otimes|\phi'\rangle\langle\phi'|$ where $|\phi'\rangle = \cos\phi_1|0\rangle + e^{i\phi_2}\sin\phi_1|1\rangle$. Then, we have

$$\mathbb{H}_2(B|F)_\rho = -\min_{\sigma_F}\log_2 \mathrm{Tr}\left\{\left((I_B\otimes\sigma_F)^{-\frac{1}{4}}\left(\frac{I}{2}\otimes|\phi'\rangle\langle\phi'|\right)(I_B\otimes\sigma_F)^{-\frac{1}{4}}\right)^2\right\} \tag{37}$$

$$= -\min_{\sigma_F} \log_2 \mathrm{Tr}\left(\frac{I_B}{4}\right) \mathrm{Tr}\left\{\left(\sigma_F^{-\frac{1}{4}}|\phi'\rangle\langle\phi'|\sigma_F^{-\frac{1}{4}}\right)^2\right\} \tag{38}$$

$$= 1 - 2\min_{\sigma_F} \log_2 \langle\phi'|\sigma_F^{-\frac{1}{2}}|\phi'\rangle \geqslant 0. \tag{39}$$

Therefore, $\max_{\sigma_F} \mathbb{H}_2(B|F)_\rho = 1$ is attained when $\phi_1 = \phi_2 = 0$ and $\sigma_F = (1/2)[(1 + r_3)|0\rangle\langle 0| + (1 - r_3)|1\rangle\langle 1|]$ for $r_3 \to 1$.
As a result, the lower bound (24) reads

$$1 - \frac{1}{n} g\left(\sqrt{\frac{\varepsilon}{2}} - \delta_\star\right) - \frac{4}{n}\log_2\frac{1}{\delta_\star} - \frac{2}{n}. \tag{40}$$

(iv) $\alpha_x = \alpha_y = \frac{\pi}{2}$, $\alpha_z = 0$ ($U = DCNOT$). In this case

$$\rho_{BF} = \begin{pmatrix} \frac{1}{2}\cos^2(\phi_1) & \frac{1}{4}ie^{i\phi_2}\sin(2\phi_1) & 0 & 0 \\ -\frac{1}{4}ie^{-i\phi_2}\sin(2\phi_1) & \frac{1}{2}\sin^2(\phi_1) & 0 & 0 \\ 0 & 0 & \frac{1}{2}\cos^2(\phi_1) & -\frac{1}{4}ie^{i\phi_2}\sin(2\phi_1) \\ 0 & 0 & \frac{1}{4}ie^{-i\phi_2}\sin(2\phi_1) & \frac{1}{2}\sin^2(\phi_1) \end{pmatrix}. \tag{41}$$

This can also be written as $\rho_{BF} = \frac{I}{2} \otimes |\phi'\rangle\langle\phi'|$ where $|\phi'\rangle = \cos\phi_1|0\rangle + ie^{i\phi_2}\sin\phi_1|1\rangle$. Then we can repeat the reasoning of case (iii) and arrive to the lower bound (24) as

$$1 - \frac{1}{n} g\left(\sqrt{\frac{\varepsilon}{2}} - \delta_\star\right) - \frac{4}{n}\log_2\frac{1}{\delta_\star} - \frac{2}{n}. \tag{42}$$

Summarizing, for I and CNOT no quantum information can be retrieved according to the used figure of merit. Instead for SWAP and DCNOT maximal quantum information retrieval (1 qubit) can be approached by increasing the number of shots n even with a fixed value of error ε.

3.3. Evaluation on the edges

We now extend, with the help of numerics, the analysis of the figure of merit along the edges of the tetrahedron.

In the cases analyzed in section 3.2 the relevant part is given by $\max_{\sigma_F} \mathbb{H}_2(B|F)_\rho$. The continuity of $\mathbb{H}_2(B|F)_\rho$ (see appendix B), hence its uniform continuity, allows us to reliable sampling discrete points for plotting its behavior along edges of the tetrahedron of figure 2. The results are summarized in figure 3.

We can see that, while along the edge IC the quantity $\max_{\sigma_F} \mathbb{H}_2(B|F)_\rho$ remains always zero, along the edges IS, ID (dotted curve), it becomes nonzero only after a certain (threshold) value of $|\boldsymbol{\alpha}|$ ($|\boldsymbol{\alpha}| \approx \pi/3.4$). Instead, along the edges CD, CS (dashed-dotted curve), it smoothly increases since the CNOT. Lastly, for the edge DS it is constant and equal to 1. This latter result is inline with the fact that on the edge DS the output $\mathcal{N}_{\boldsymbol{\phi}}^{E\to B}(\boldsymbol{\theta})$, for $\boldsymbol{\phi} = |0\rangle\langle 0|$ or $|1\rangle\langle 1|$, simply gives a rotated version of the state $\boldsymbol{\theta}$, thus allowing its perfect recovery.

Overall the results indicate that there could be a nonzero volume of unitaries around identity for which quantum information retrieval would not be possible. The use of conditional is due to the fact that $\mathbb{H}_2(B|F)_\rho$ is a lower bound to the one-shot capacity.

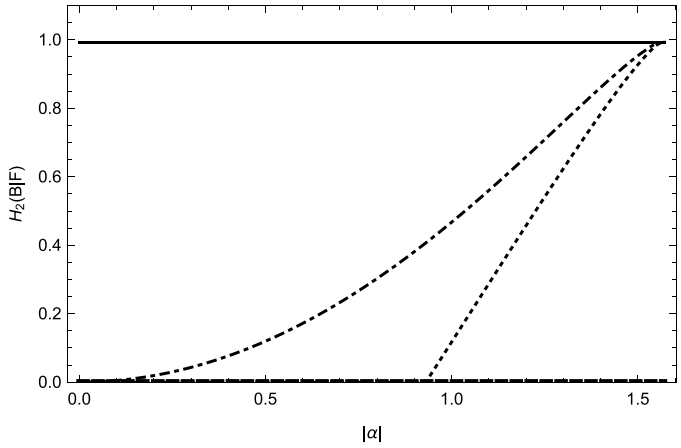

Figure 3. Quantity $\mathbb{H}_2(B|F)_\rho$ evaluated along the various edges of the tetrahedron as function of the parameter $|\boldsymbol{\alpha}|$. Dashed curve corresponds to the edge IC; dotted curve to the edges IS and ID; dashed-dotted curve to the edges CD and CS; solid curve to the edge DS.

4. Quantum state estimation

By referring to figure 1, we now consider the goal of estimating parameters $\boldsymbol{\theta} = (r, \theta_1, \theta_2) \in \Theta$, where $\Theta = [0 \leqslant r \leqslant \frac{1}{2}, 0 \leqslant \theta_1 \leqslant \pi, 0 \leqslant \theta_2 \leqslant 2\pi]$, characterizing the environment state

$$\boldsymbol{\theta} = \frac{1}{2} I + r \sin\theta_1 \cos\theta_2 \sigma_x + r \sin\theta_1 \sin\theta_2 \sigma_y + r \cos\theta_2 \sigma_z. \tag{43}$$

Here $\sigma_x, \sigma_y, \sigma_z$ are the Pauli matrices. The estimation should be done by means of the channel output $\mathscr{N}_{\boldsymbol{\theta}}(\phi)$. As a figure of merit we will derive a Bayesian version of the quantum Cramer–Rao bound following the classical bound [20].

4.1. Lower bound

Let $\{p(x;\boldsymbol{\theta})\}_{\boldsymbol{\theta}\in\Theta}$ be a family of probability density functions on a sample space $\mathcal{X}$. Any unbiased estimator $\hat{\boldsymbol{\theta}}$ of $\boldsymbol{\theta}$ satisfies the multivariate Cramer–Rao inequality:

$$\mathbb{E}_p \left[\left(\hat{\boldsymbol{\theta}} - \boldsymbol{\theta} \right) \left(\hat{\boldsymbol{\theta}} - \boldsymbol{\theta} \right)^{\mathrm{T}} \right] \geqslant \mathscr{I}(\boldsymbol{\theta})^{-1}, \tag{44}$$

where $\mathbb{E}_p$ denotes the expectation with respect to $p(x;\boldsymbol{\theta})$, $\mathscr{I}(\boldsymbol{\theta})$ is the classical Fisher information, and $\mathbb{E}_p[(\hat{\boldsymbol{\theta}} - \boldsymbol{\theta})(\hat{\boldsymbol{\theta}} - \boldsymbol{\theta})^{\mathrm{T}}]$ is the covariance matrix of $\hat{\boldsymbol{\theta}}$.

After assigning a proper prior probability distribution π to $\boldsymbol{\theta}$ and taking the expectation of equation (44), we can get the simplest Bayesian Cramer–Rao bound:

$$\mathbb{E}_\pi \left\{ \mathbb{E}_p \left[\left(\hat{\boldsymbol{\theta}} - \boldsymbol{\theta} \right) \left(\hat{\boldsymbol{\theta}} - \boldsymbol{\theta} \right)^{\mathrm{T}} \right] \right\} \geqslant \mathbb{E}_\pi \left\{ [\mathscr{I}(\boldsymbol{\theta})] \right\}^{-1}. \tag{45}$$

We assume the parameters r, $\boldsymbol{\theta}_1$ and $\boldsymbol{\theta}_2$ independent, and distributed according to the measure [26] $\pi(\boldsymbol{\theta}) d\boldsymbol{\theta} = \sin\frac{\theta_1}{2} \mathrm{d}r \mathrm{d}\theta_1 \mathrm{d}\theta_2 / (2\pi)$. Taking into account that quantum Fisher information $\mathscr{F}(\boldsymbol{\theta})$ upper bounds the classical Fisher information $\mathscr{I}(\boldsymbol{\theta})$, we get

$$\mathbb{E}_\pi\left\{\mathbb{E}_p\left[\left(\hat{\boldsymbol{\theta}}-\boldsymbol{\theta}\right)\left(\hat{\boldsymbol{\theta}}-\boldsymbol{\theta}\right)^{\mathrm{T}}\right]\right\} \geqslant \left\{\mathbb{E}_\pi\left[\mathscr{I}\left(\boldsymbol{\theta}\right)\right]\right\}^{-1}$$
$$= \frac{4}{\int_\Theta \mathrm{tr}\left\{\mathscr{I}\left(\boldsymbol{\theta}\right)\right\}\pi\left(\boldsymbol{\theta}\right)\mathrm{d}\boldsymbol{\theta}}$$
$$\geqslant \frac{4}{\int_\Theta \mathrm{tr}\left\{\mathscr{F}\left(\boldsymbol{\theta}\right)\right\}\pi\left(\boldsymbol{\theta}\right)\mathrm{d}\boldsymbol{\theta}}. \tag{46}$$

Then the quantity of interest for us becomes

$$F_{\boldsymbol{\phi}} := \int_\Theta \mathrm{tr}\left\{\mathscr{F}\left(\boldsymbol{\theta}\right)\right\}\pi\left(\boldsymbol{\theta}\right)\mathrm{d}\boldsymbol{\theta}, \tag{47}$$

where the subscript emphasizes its dependence from the input state $\boldsymbol{\phi}$ of the A system.

Its maximum overall states $\boldsymbol{\phi}$ will be denoted by $\overline{F}$. Due to the convexity of the Fisher information, the optimization can be restricted to pure states of the form

$$|\boldsymbol{\phi}\rangle = \cos\frac{\phi_1}{2}|0\rangle + e^{i\phi_2}\sin\frac{\phi_1}{2}|1\rangle, \tag{48}$$

where $\phi_1 \in [0,\pi]$ and $\phi_2 \in [0,2\pi]$.

From [27], we know that the basis-independent expression of quantum Fisher information for a single-qubit mixed state $\rho(\boldsymbol{\theta})$ reads

$$\mathscr{F}_{ab} = \mathrm{tr}\left[\left(\partial_a\rho\right)\left(\partial_b\rho\right)\right] + \frac{\mathrm{tr}\left[\rho\left(\partial_a\rho\right)\rho\left(\partial_b\rho\right)\right]}{\det\left(\rho\right)}, \tag{49}$$

where $\partial_a\rho = \partial\rho/\partial\theta_a$. For a pure qubit state equation (49) reduces to

$$\mathscr{F}_{ab} = 2\mathrm{tr}\left[\left(\partial_a\rho\right)\left(\partial_b\rho\right)\right]. \tag{50}$$

4.2. Evaluation on the vertices

We now work out the calculation of $\overline{F}$ for the four cases of unitaries in the vertices of the tetrahedron (see figure 2).

(i) $\alpha_x = \alpha_y = \alpha_z = 0$ ($U = I$). In this case equation (7) reduces to the identity and hence $\mathscr{F} = 0$ for all input $|\boldsymbol{\phi}\rangle$. As a consequence $\overline{F} = 0$.

(ii) $\alpha_x = \frac{\pi}{2}$, $\alpha_y = \alpha_z = 0$ ($U = CNOT$). In this case

$$\mathscr{N}_{\boldsymbol{\theta}}\left(\boldsymbol{\phi}\right) = \frac{1}{2} + r\sin\theta_1\cos\theta_2\sin\phi_1\sin\phi_2|0\rangle\langle 0|$$
$$+ \frac{1}{2}\sin\phi_1\cos\phi_2 + ir\sin\theta_1\cos\theta_2\cos\phi_1|0\rangle\langle 1|$$
$$+ \frac{1}{2}\sin\phi_1\cos\phi_2 - ir\sin\theta_1\cos\theta_2\cos\phi_1|1\rangle\langle 0|$$
$$+ \frac{1}{2} - r\sin\theta_1\cos\theta_2\sin\phi_1\sin\phi_2|1\rangle\langle 1|. \tag{51}$$

Then

$$\mathscr{F}_{\theta_1,\theta_1} = \frac{4r^2\cos^2\theta_1\cos^2\theta_2\left(1-\sin^2\phi_1\cos^2\phi_2\right)}{1-4r^2\sin^2\theta_1\cos^2\theta_2},$$
$$\mathscr{F}_{\theta_2,\theta_2} = \frac{4r^2\sin^2\theta_1\sin^2\theta_2\left(1-\sin^2\phi_1\cos^2\phi_2\right)}{1-4r^2\sin^2\theta_1\cos^2\theta_2},$$
$$\mathscr{F}_{r,r} = \frac{4\sin^2\theta_1\cos^2\theta_2\left(1-\sin^2\phi_1\cos^2\phi_2\right)}{1-4r^2\sin^2\theta_1\cos^2\theta_2}. \tag{52}$$

The maximum of

$$F_{\boldsymbol{\phi}} = \int_{\Theta} \mathrm{Tr}\left\{\mathscr{F}(\boldsymbol{\theta})\right\}\pi(\boldsymbol{\theta})\,\mathrm{d}\boldsymbol{\theta}. \tag{53}$$

is achieved for $\phi_1 = 0,\pi$ or $\phi_2 = \frac{\pi}{2}, \frac{3\pi}{2}$, In this case it is $\overline{F} = 1.76108$.

(iii) $\alpha_x = \alpha_y = \alpha_z = \frac{\pi}{2}$ ($U = SWAP$). In this case

$$\mathscr{N}_{\boldsymbol{\theta}}(\boldsymbol{\phi}) = \left(\frac{1}{2} + r\cos\theta_1\right)|0\rangle\langle 0| + re^{-i\theta_2}\sin\theta_1|0\rangle\langle 1| + re^{i\theta_2}\sin\theta_1|1\rangle\langle 0| + \left(\frac{1}{2} - r\cos\theta_1\right)|1\rangle\langle 1|. \tag{54}$$

Then

$$\mathscr{F}_{\theta_1,\theta_1} = 4r^2, \tag{55}$$

$$\mathscr{F}_{\theta_2,\theta_2} = 4r^2\sin^2\theta_1, \tag{56}$$

$$\mathscr{F}_{r,r} = \frac{4}{1-4r^2}. \tag{57}$$

Clearly

$$\int_{\Theta} \mathrm{Tr}\left\{\mathscr{F}(\boldsymbol{\theta})\right\}\pi(\boldsymbol{\theta})\,\mathrm{d}\boldsymbol{\theta}, \tag{58}$$

diverges, meaning that for any state $\boldsymbol{\phi}$ we will have a good estimation on average.

(iv) $\alpha_x = \alpha_y = \frac{\pi}{2}$, $\alpha_z = 0$ ($U = DCNOT$). In this case

$$\mathscr{N}_{\boldsymbol{\theta}}(\boldsymbol{\phi}) = \left(\frac{1}{2} + r\cos\theta_1\right)|0\rangle\langle 0| + ie^{-i\theta_2}r\sin\theta_1\cos\phi_1|0\rangle\langle 1| - ie^{i\theta_2}r\sin\theta_1\cos\phi_1|1\rangle\langle 0| + \left(\frac{1}{2} - r\cos\theta_1\right)|1\rangle\langle 1|. \tag{59}$$

Then

$$\mathscr{F}_{\theta_1,\theta_1} = \frac{4r^2\left(\sin^2\theta_1 - \left(4r^2-\cos^2\theta_1\right)\cos^2\phi_1\right)}{1-4r^2\left(\cos^2\theta_1 + \sin^2\theta_1\cos^2\phi_1\right)}, \tag{60}$$

$$\mathscr{F}_{\theta_2,\theta_2} = 4r^2 \sin^2\theta_1 \cos^2\phi_1, \tag{61}$$

$$\mathscr{F}_{r,r} = \frac{4\left(\cos^2\theta_1 + \sin^2\theta_1\cos^2\phi_1\right)}{1-4r^2\left(\cos^2\theta_1 + \sin^2\theta_1\cos^2\phi_1\right)}. \tag{62}$$

Notice that these three terms are non negative, hence maximizing (47) is equivalent to maximize them. However, their derivative with respect to $\cos^2\phi_1$ never nullify. Hence, the maximum is at the extreme points. Actually it is easy to see that it occurs for $\cos^2\phi_1 = 1$. As a consequence we will have

$$\overline{F} = \int_\Theta \left[4r^2 + 4r^2\sin^2\theta_1 + \frac{4}{1-4r^2}\right]\pi(\boldsymbol{\theta})\,\mathrm{d}\boldsymbol{\theta}, \tag{63}$$

which diverges, likewise the case of SWAP.

The fact that $\overline{F}$ diverges for DCNOT and SWAP is in line with the results in section 3 where the bound for one-shot capacity in these cases turns out to be (close to) 1. In other words for DCNOT and SWAP the environment state can be estimated with perfect accuracy or analogously it can be transmitted with maximum reliability to the B system.

Also for identity we have concordance between the two approaches. In fact the environment state can be estimated with total inaccuracy or analogously it can be transmitted to the B system in a total unreliable way.

The situation is slightly different for CNOT, since according to the one-shot capacity approach it behaves like identity, while state environment estimation can be done with a finite average error.

4.3. Evaluation on the edges

We now extend, with the help of numerics, the analysis of the figure of merit along the edges of the tetrahedron.

The continuity of the average quantum Fisher information (see appendix C), hence its uniform continuity, allows us to reliable sampling discrete points for plotting its behavior along edges of the tetrahedron of figure 2. The results are summarized in figure 4.

We can see that along the edges (IC), (ID), (IS) the quantity $\overline{F}$ smoothly increases from zero, remaining finite only for (IC). Instead for (CS and CD) it starts from a finite positive value and then diverges. These results indicate that only for identity quantum information retrieval would not be possible. For all other unitaries it would be possible, although in some cases with a finite average error.

However, from figure 4 it is left out the edge (SD). On that edge, we have (7) as

$$U = \begin{pmatrix} e^{-\frac{iz}{2}} & 0 & 0 & 0 \\ 0 & 0 & -ie^{\frac{iz}{2}} & 0 \\ 0 & -ie^{\frac{iz}{2}} & 0 & 0 \\ 0 & 0 & 0 & e^{-\frac{iz}{2}} \end{pmatrix}. \tag{64}$$

Therefore

$$\mathscr{N}_{\boldsymbol{\theta}}(\boldsymbol{\phi}) = \left(\frac{1}{2} + r\cos\theta_1\right)|0\rangle\langle 0| + re^{-i\theta_2}\sin\theta_1\left(\sin\alpha_z + i\cos\alpha_z\cos\phi_1\right)|0\rangle\langle 1|$$

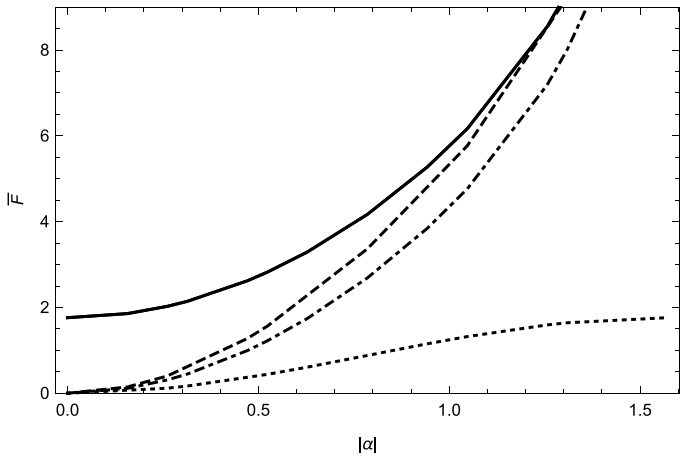

Figure 4. Quantity $\overline{F}$ evaluated along the various edges of the tetrahedron as function of the parameter $|\boldsymbol{\alpha}|$. Curves from bottom to top refer respectively to the edges (IC), (ID), (IS), (CS and CD). The edge (DS) is not represented because along it, the value of $\overline{F}$ is infinity.

$$+ re^{i\theta_2}\sin\theta_1\left(\sin\alpha_z - i\cos\alpha_z\cos\left(\phi_1\right)\right)|1\rangle\langle 0| + \left(\frac{1}{2} - r\cos\theta_1\right)|1\rangle\langle 1|, \tag{65}$$

and

$$\mathscr{F}_{\theta_1,\theta_1} = \frac{4r^2\left(1-4r^2+\left(4r^2-\cos^2\theta_1\right)\sin^2\phi_1\cos^2\alpha_z\right)}{1-4r^2\left(1-\cos^2\alpha_z\sin^2\theta_1\sin^2\phi_1\right)}, \tag{66}$$

$$\mathscr{F}_{\theta_2,\theta_2} = 4r^2\sin^2\theta_1\left(1-\cos^2\alpha_z\sin^2\phi_1\right), \tag{67}$$

$$\mathscr{F}_{r,r} = \frac{4\left(1-\cos^2\alpha_z\sin^2\theta_1\sin^2\phi_1\right)}{1-4r^2\left(1-\cos^2\alpha_z\sin^2\theta_1\sin^2\phi_1\right)}. \tag{68}$$

$F_{\boldsymbol{\phi}}$ does not have extrema with respect to α_z inside the interval $\left(0,\frac{\pi}{2}\right)$, and we know that on the two ends of the interval it has the same maximum value. Thus, we can conclude, that on the edge SD we have a constant infinite value of $\overline{F}$ (allowing quantum information recovering with zero average error), that originates form the fact that the output $\mathscr{N}_{\boldsymbol{\phi}}^{E\to B}(\boldsymbol{\theta})$, for $\boldsymbol{\phi} = |0\rangle\langle 0|$ or $|1\rangle\langle 1|$, simply gives a rotated version of the state $\boldsymbol{\theta}$ (as discussed in section 3.3).

5. Conclusion

In conclusion, we have addressed the problem of reading quantum information by a quantum probe, thus going beyond the standard paradigm that confines quantum reading to the retrieval of classical information. As a model of quantum memory we used environment parametrized quantum channels arising from two-qubit unitaries. Since these unitaries lie in a tetrahedron in $\mathbb{R}^3$, we characterized those on the edges to have general insights. To this end, we used a lower bound to the one-shot quantum capacity of the channel connecting the environment with the output of the main system (probe) as well as a Bayesian version of the quantum Cramer–Rao bound for the initial environment state. We remark that while the first also showed the behavior vs the number n of shots, the second just refers to one-shot, Notwithstanding, the results of

the first are more restrictive. In fact, according to the first figure of merit, there should be a nonzero volume of unitaries around identity for which quantum information retrieval would not be possible. Instead, the second shows that only for identity quantum information retrieval would not be possible. For all other unitaries it would be possible, although in some cases with a finite average error.

This difference of behavior between the two figures of merit (to most striking of which occurs for CNOT) should be ascribed to the non tightness of the used lower bound for to the one-shot quantum capacity.

In future, besides investigating also the unitaries inside the tetrahedron, we plan to characterize spatial arrays of the presented model to figure out the performance of realistic quantum memories. A fact that can be useful for applications in quantum cryptography as well as in quantum computation.

Data availability statement

No new data were created or analyzed in this study.

Appendix A. Value of $\delta_\star$

$$\begin{aligned}\delta_\star = \frac{13\sqrt{\varepsilon}}{15\sqrt{2}} &- \frac{\left(1+i\sqrt{3}\right)\sqrt[3]{\sqrt{2\varepsilon^3}+\sqrt{1728\varepsilon^2+715392\varepsilon-5971968}+648\sqrt{2\varepsilon}}}{30\ 2^{2/3}} \\ &- \frac{\left(1-i\sqrt{3}\right)(\varepsilon+144)}{30\sqrt[3]{2}\sqrt[3]{\sqrt{2\varepsilon^3}+\sqrt{1728\varepsilon^2+715392\varepsilon-5971968}+648\sqrt{2\varepsilon}}}.\end{aligned} \tag{69}$$

Appendix B. Continuity of lower bound on the one-shot quantum capacity

Let us consider

$$\rho_{BF} = \left(\mathrm{id}_{A\to B}\otimes\left(\mathscr{N}_{E\to B}\right)^c\right)(\Phi_{AE}), \tag{70}$$

$$\rho'_{BF} = \left(\mathrm{id}_{A\to B}\otimes\left(\mathscr{N}'_{E\to B}\right)^c\right)(\Phi_{AE}), \tag{71}$$

where $\mathscr{N}$ and $\mathscr{N}'$ refer respectively to the unitaries $U_{\boldsymbol{\alpha}}$ and $U_{\boldsymbol{\alpha}'}$. Then, we have

$$\begin{aligned}\left\|\rho_{BF}-\rho'_{BF}\right\|_1 &= \left\|\left(\mathrm{id}_{A\to B}\otimes\left(\left(\mathscr{N}_{E\to B}\right)^c-\left(\mathscr{N}'_{E\to B}\right)^c\right)\right)(\Phi_{AE})\right\|_1 && (72)\\ &\leqslant \left\|\left(\mathscr{N}_{E\to B}\right)^c-\left(\mathscr{N}'_{E\to B}\right)^c\right\|_\diamond && (73)\\ &\leqslant C_1\left\|U_{\boldsymbol{\alpha}}-U_{\boldsymbol{\alpha}'}\right\|_\infty && (74)\\ &\leqslant C_2\left\|\boldsymbol{\alpha}-\boldsymbol{\alpha}'\right\|_{\mathbb{R}^3}, && (75)\end{aligned}$$

where $C_i < +\infty$ are positive constants. Furthermore, $\|\cdot\|_\diamond$ is the diamond norm and relation (74) comes from [28].

Now, for a given $\varepsilon = \|\boldsymbol{\alpha} - \boldsymbol{\alpha}'\|_{\mathbb{R}^3} > 0$, it is shown [29] that

$$\left|\mathbb{H}_2\left(B|F\right)_\rho - \mathbb{H}_2\left(B|F\right)_{\rho'}\right| \leqslant \log_2\left(1+\sqrt{\varepsilon}\right) + 3\log_2\left(1 + 64\sqrt[3]{\varepsilon} - \frac{\sqrt{\varepsilon}}{\sqrt[3]{1+\sqrt{\varepsilon}}}\right), \tag{76}$$

where $\mathbb{H}_2(B|F)_\rho$ is defined in (21).

Appendix C. Continuity of average quantum Fisher information

Let us denote by $\boldsymbol{\alpha}$ the parameters vector characterizing the unitary.

$$\left|\overline{F}_{\boldsymbol{\alpha}} - \overline{F}_{\boldsymbol{\alpha}'}\right| = \left|\max_{\boldsymbol{\phi}} \int_\Theta \mathrm{Tr}\left\{\mathscr{F}_{\boldsymbol{\alpha}}\left(\boldsymbol{\theta},\boldsymbol{\phi}\right)\right\}\pi\left(\boldsymbol{\theta}\right)\mathrm{d}\boldsymbol{\theta} - \max_{\boldsymbol{\phi}} \int_\Theta \mathrm{Tr}\left\{\mathscr{F}_{\boldsymbol{\alpha}'}\left(\boldsymbol{\theta},\boldsymbol{\phi}\right)\right\}\pi\left(\boldsymbol{\theta}\right)\mathrm{d}\boldsymbol{\theta}\right| \tag{77}$$

$$\leqslant \max_{\boldsymbol{\phi},\boldsymbol{\phi}'}\left|\int_\Theta \mathrm{Tr}\left\{\mathscr{F}_{\boldsymbol{\alpha}}\left(\boldsymbol{\theta},\boldsymbol{\phi}\right)\right\}\pi\left(\boldsymbol{\theta}\right)\mathrm{d}\boldsymbol{\theta} - \int_\Theta \mathrm{Tr}\left\{\mathscr{F}_{\boldsymbol{\alpha}'}\left(\boldsymbol{\theta},\boldsymbol{\phi}'\right)\right\}\pi\left(\boldsymbol{\theta}\right)\mathrm{d}\boldsymbol{\theta}\right| \tag{78}$$

$$\leqslant \max_{\boldsymbol{\phi},\boldsymbol{\phi}'}\int_\Theta \left|\mathrm{Tr}\left\{\mathscr{F}_{\boldsymbol{\alpha}}\left(\boldsymbol{\theta},\boldsymbol{\phi}\right)\right\} - \mathrm{Tr}\left\{\mathscr{F}_{\boldsymbol{\alpha}'}\left(\boldsymbol{\theta},\boldsymbol{\phi}'\right)\right\}\right|\pi\left(\boldsymbol{\theta}\right)\mathrm{d}\boldsymbol{\theta} \tag{79}$$

$$\leqslant C_1 \max_{\boldsymbol{\theta},\boldsymbol{\phi},\boldsymbol{\phi}'}\left|\mathrm{Tr}\left\{\mathscr{F}_{\boldsymbol{\alpha}}\left(\boldsymbol{\theta},\boldsymbol{\phi}\right)\right\} - \mathrm{Tr}\left\{\mathscr{F}_{\boldsymbol{\alpha}'}\left(\boldsymbol{\theta},\boldsymbol{\phi}'\right)\right\}\right| \tag{80}$$

$$\leqslant C_2 \max_{\boldsymbol{\theta},\boldsymbol{\theta}',\boldsymbol{\phi},\boldsymbol{\phi}'}\left|\mathrm{Tr}\left\{\mathscr{F}_{\boldsymbol{\alpha}}\left(\boldsymbol{\theta},\boldsymbol{\phi}\right)\right\} - \mathrm{Tr}\left\{\mathscr{F}_{\boldsymbol{\alpha}'}\left(\boldsymbol{\theta}',\boldsymbol{\phi}'\right)\right\}\right| \tag{81}$$

$$\leqslant C_3 \max_{\boldsymbol{\theta},\boldsymbol{\theta}',\boldsymbol{\phi},\boldsymbol{\phi}'}\left\|\mathscr{N}_{\boldsymbol{\theta}}^{\boldsymbol{\alpha}}\left(\boldsymbol{\phi}\right) - \mathscr{N}_{\boldsymbol{\theta}'}^{\boldsymbol{\alpha}'}\left(\boldsymbol{\phi}'\right)\right\|_1 \tag{82}$$

$$= C_3 \max_{\boldsymbol{\theta},\boldsymbol{\theta}',\boldsymbol{\phi},\boldsymbol{\phi}'}\left\|\mathrm{Tr}_E\left[U_{\boldsymbol{\alpha}}\boldsymbol{\phi}\otimes\boldsymbol{\theta}U_{\boldsymbol{\alpha}}^\dagger\right] - \mathrm{Tr}_E\left[U_{\boldsymbol{\alpha}'}\boldsymbol{\phi}'\otimes\boldsymbol{\theta}'U_{\boldsymbol{\alpha}'}^\dagger\right]\right\|_1 \tag{83}$$

$$\leqslant C_4 \max_{\boldsymbol{\theta},\boldsymbol{\theta}',\boldsymbol{\phi},\boldsymbol{\phi}'}\left\|U_{\boldsymbol{\alpha}}\boldsymbol{\phi}\otimes\boldsymbol{\theta}U_{\boldsymbol{\alpha}}^\dagger - U_{\boldsymbol{\alpha}'}\boldsymbol{\phi}'\otimes\boldsymbol{\theta}'U_{\boldsymbol{\alpha}'}^\dagger\right\|_1 \tag{84}$$

$$\leqslant C_5\left\|U_{\boldsymbol{\alpha}} - U_{\boldsymbol{\alpha}'}\right\|_\infty \tag{85}$$

$$\leqslant C_6\left\|\boldsymbol{\alpha} - \boldsymbol{\alpha}'\right\|_{\mathbb{R}^3}, \tag{86}$$

where $C_i < +\infty$ are positive constants. In going from (81) to (82) we used the continuity of the Fisher information [30]. In going from (83) to (84) we used the property that discarding a system cannot increase the norm [31].

ORCID iDs

Samad Khabbazi Oskouei https://orcid.org/0000-0002-5244-7918
Stefano Mancini https://orcid.org/0000-0002-3797-3987
Milajiguli Rexiti https://orcid.org/0000-0002-3864-7083

References

[1] Pirandola S 2011 Quantum reading of a classical digital memory *Phys. Rev. Lett.* **106** 090504
[2] Pirandola S 2021 On quantum reading, quantum illumination and other notions *IOPSciNotes* **2** 015203

[3] Gilchrist A, Langford N K and Nielsen M A 2005 Distance measures to compare real and ideal quantum processes *Phys. Rev.* A **71** 062310
[4] Sacchi M 2005 Optimal discrimination of quantum operations *Phys. Rev.* A **71** 062340
[5] Wang G and Ying M 2006 Unambiguous discrimination among quantum operations *Phys. Rev.* A **73** 042301
[6] Hayashi M 2009 Discrimination of two channels by adaptive methods and its application to quantum system *IEEE Trans. Inf. Theory* **55** 3807
[7] Ortolano G, Ruo-Berchera I and Predazzi E 2019 Quantum enhanced imaging of nonuniform refractive profiles *Int. J. Quantum Inf.* **17** 1941010
[8] Zhuang Q 2023 Quantum advantage on the radar *Nat. Phys.* **19** 1384–5
[9] de Andrade R B, Kerdoncuff H, Berg-Sørensen K, Gehring T, Lassen M and Andersen U L 2020 Quantum-enhanced continuous-wave stimulated Raman scattering spectroscopy *Optica* **7** 470
[10] Spedalieri G 2015 Cryptographic aspects of quantum reading *Entropy* **17** 2218
[11] Khabbazi Oskouei S, Mancini S and Winter A 2022 Capacities of Gaussian quantum channels with passive environment assistance *IEEE Trans. Inf. Theory* **68** 339
[12] Das S and Wilde M M 2019 Quantum reading capacity: general definition and bounds *IEEE Trans. Inf. Theory* **65** 7566
[13] Rexiti M and Mancini S 2017 Estimation of two-qubit interactions through channels with environment assistance *Int. J. Quantum Inf.* **15** 1750053
[14] Karumanchi S, Mancini S, Winter A and Yang D 2016 Classical Capacities of quantum channels with environment assistance *Problems Inf. Trans.* **52** 214
[15] Karumanchi S, Mancini S, Winter A and Yang D 2016 Quantum channel capacities with passive environment assistance *IEEE Trans. Inf. Theory* **62** 1733
[16] Baüml S, Das S and Wilde M M 2018 Fundamental limits on the capacities of bipartite quantum interactions *Phys. Rev. Lett.* **121** 250504
[17] Das S, Baüml S and Wilde M M 2020 Entanglement and secret-key-agreement capacities of bipartite quantum interactions and rea-only memory devices *Phys. Rev.* A **101** 012344
[18] Buscemi F and Datta N 2010 The quantum capacity of channels with arbitrarily correlated noise *IEEE Trans. Inf. Theory* **56** 1447
[19] Pfister C, Rol M A, Mantri A, Tomamichel M and Wehner S 2018 Capacity estimation and verification of quantum channels with arbitrarily correlated errors *Nat. Commun.* **9** 27
[20] Gill R D and Levit B Y 1995 Applications of the Van Trees inequality: a Bayesian Cramér-Rao bound *Bernoulli* **1** 59
[21] Rexiti M and Mancini S 2019 Adversarial vs cooperative quantum estimation *Quantum Inf. Process.* **18** 102
[22] Pirandola S, Lupo C, Giovannetti V, Mancini S and Braunstein S L 2011 Quantum reading capacity *New J. Phys.* **13** 113012
[23] Wilde M M 2020 Coherent quantum channel discrimination *Proc. 2020 IEEE Int. Symp. on Information Theory* pp 1921–6
[24] Kraus B and Cirac J I 2001 Optimal creation of entanglement using a two-qubit gate *Phys. Rev.* A **63** 062309
[25] Tomamichel M 2016 *Quantum Information Processing With Finite Resources: Mathematical Foundations (Springer Briefs in Mathematical Physics)* (Springer) (https://doi.org/10.1007/978-3-319-21891-5)
[26] Zyczkowski K and Sommers H J 2001 Induced measures in the space of mixed quantum states *J. Phys. A: Math. Gen.* **34** 7111
[27] Liu J, Yuan H, Lu X-M and Wang X 2020 Quantum Fisher information matrix and multiparameter estimation *J. Phys. A: Math Theor.* **53** 023001
[28] Kretschmann D, Schlingemann D and Werner R F 2008 The information-disturbance tradeoff and the continuity of Stinespring's representation *IEEE Trans. Inf. Theory* **54** 1708
[29] Marwah A and Dupuis F 2022 Uniform continuity bound for sandwiched Rényi conditional entropy *J. Math. Phys.* **63** 052201
[30] Rezakhani A T and Alipour S 2019 Continuity of the quantum Fisher information *Phys. Rev.* A **100** 032317
[31] Rastegin A E 2012 Relations for certain symmetric norms and anti-norms before and after partial trace *J. Stat. Phys.* **148** 1040